This document is the postprint version of a published work that appeared in final form in Peptide Science, after peer review and technical editing by the publisher. To access the final edited and published work, see:

https://onlinelibrary.wiley.com/doi/10.1002/pep2.24081

The Several Facets of Trichogin GA IV: High Affinity Tb (III) Binding Properties. A Spectroscopic and Molecular Dynamics Simulation Study

Emanuela Gatto,*[1] Maria Elena Palleschi,[1] Beatrice Zangrilli,[1] Marta De Zotti,[2] Benedetta Di Napoli,[1] Antonio Palleschi,[1] Claudia Mazzuca,[1] Fernando Formaggio,[2] Claudio Toniolo,[2] Mariano Venanzi[1]

[1]Department of Chemical Sciences and Technologies, University of Rome "Tor Vergata", 00133 Rome (Italy)

[2]Institute of Biomolecular Chemistry, Padova Unit, CNR, Department of Chemistry, University of Padova, 35131 Padova (Italy)

Correspondence

Emanuela Gatto, Department of Chemical Sciences and Technologies, University of Rome "Tor Vergata", 00133 Rome (Italy)

E-mail: emanuela.gatto@uniroma2.it

ABSTRACT

Trichogin GA IV (TrGA) is an antimicrobial peptide isolated from *Trichoderma longibrachiatum*. The amino acid sequence of TrGA is rather peculiar, because it is characterized by three Aib and four Gly residues, which confer unique dynamic and structural properties. In a previous study, we found that TrGA shows excellent binding properties to Ca(II) and lanthanide Gd(III) ions in acetonitrile solutions. Within the lanthanide ions, Tb(III) ions possess fascinating optical characteristics, such as luminescence which greatly improves after coordination. Here, we present the results of our spectroscopic and molecular dynamics investigations on the Tb(III) ion-binding properties of an N^{α}-Fmoc functionalized analog of Trichogin GA IV (F0TrOMe). The high Tb(III) ion- F0TrOMe affinity, together with the proteolytic resistance and membrane affinity of the natural compound, confers to this system potentially promising applications in several fields, such as bioimaging and bioanalytical assays.

KEYWORDS

circular dichroism, luminescence, ion-peptide complexes, lipopeptaibol antibiotic, molecular dynamics simulations
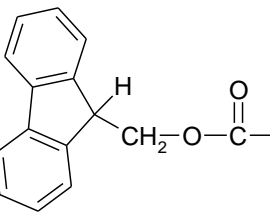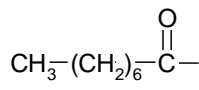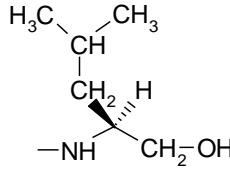
INTRODUCTION

Peptaibols are a large family of peptides isolated from soil fungi, ranging in length from 5 to 20 amino acids.[1-4] Trichogin GA IV (TrGA)[5] is an extensively studied peptaibol isolated from *Trichoderma longibrachiatum*[6] and firstly synthesized in 1994,[7] with antimicrobial and cytotoxic activity,[8] that exhibits proteolytic resistance properties.[9] The amino acid sequence of this terminally-blocked decapeptide amide (Table 1) is rather peculiar, comprising a lipophilic 1-octanoyl group at the N-terminus, an L-configured 1,2-amino alcohol (leucinol, Lol) at the C-terminus, and three α-aminoisobutyric acid (Aib) residues at positions 1, 4 and 8. The Aib residue is the prototype of an interesting class of α-amino acids characterized by a tetrasubstituted C^{α}-atom.[10] In the achiral Aib residue, a second methyl group substitutes the C^{α}-hydrogen atom (for this reason, it is also denoted α-methylalanine). Theoretical calculations have demonstrated that the C^{α}-tetrasubstitution imposes a marked restriction on the available peptide conformational ϕ, ψ space, because of unfavorable van der Waals interactions.[11-13] The associated Ramachandran plot shows few energy minima centered around the typical values of helical conformations.[14] Due to the geminal character of the double methyl substitution on the C^{α}-atom, positive and negative values of the backbone torsional angles share the same probability, resulting in Aib homo-peptides

3

with isoenergetic left- and right-handed helices. Oligopeptides rich in Aib residues preferentially attain a 3_{10}-helix conformation, while in longer peptides Aib residues promote formation of α-helical structures.[10,15-17]

TABLE 1: Primary Structures of the Trichogin GA IV Analogs Investigated and the Chemical Structures of the Fmoc and Oct Groups, and the Lol 1,2-Amino Alcohol

TrGA	Oct-Aib-Gly-Leu-Aib-Gly-Gly-Leu-Aib-Gly-Ile-Lol
TrOMe	Oct-Aib-Gly-Leu-Aib-Gly-Gly-Leu-Aib-Gly-Ile-Leu-OMe
F0TrOMe	Fmoc-Aib-Gly-Leu-Aib-Gly-Gly-Leu-Aib-Gly-Ile-Leu-OMe

Fmoc   **Oct**   **L-Lol**

In the case of TrGA, the presence of four Gly counterbalances the conformational effect of the three Aib residues, conferring unique dynamic and 3D-structural properties. In particular, the central Gly-Gly motif, at positions 5 and 6 of the sequence, is known to promote onset of a turn conformation.[5,18-21] X-Ray diffraction studies have shown that TrGA adopts in the crystal state a mixed helical conformation, with a short 3_{10}-helix segment at the N-terminus accompanied by a longer α-helical tract in the middle and C-terminal regions of the sequence.[7] Infrared (IR) absorption, nuclear magnetic resonance (NMR), and circular dichroism (CD) experiments suggested the presence of additional 3D-structures in equilibrium with the helically folded conformation.[22-24] The dynamics of a conformational transition from an elongated, helical conformation to a family of compact, folded structures, for some Trichogin analogs was characterized by us some years ago, by use of theoretical conformational analysis and time-resolved spectroscopic studies.[20,25] We have also found that in these fluorescent TrGA analogs the conformational transition from an essentially helical structure to a turn conformation may be triggered by the binding of Ca(II) and the lanthanide Gd(III) ions.[26]

Within the lanthanide ions, Tb (III) possesses intriguing optical properties such as luminescence in the visible region,[27,28] which may greatly improve after chelation, due to loss of water molecules from the ion coordination sphere (which act as a quencher).[29] The use of Tb (III) ions in biochemistry originated from their exploitation as luminescent substitutes for Ca(II) ions.[30] They have been also widely employed in studies of protein structures, due to their long lifetime emission and coordination chemistry properties.[31] In recent years, however, a widespread attention has been

devoted to luminescent metal–organic frameworks as interesting materials, based on their numerous potential applications ranging from biomedical to sensing areas and optical imaging.[32,33]

Due to the TrGA proteolytic resistance and membrane affinity, combined with the appealing properties of Tb(III) ion materials, in a previous very short contribution,[34] we have explored the possible formation of a TrGA/Tb(III) ion complex, using a TrGA fluorescent analog (F0TrOMe, Table 1)[35,36] containing the N^α-protecting group fluorenyl-9-methyloxycarbonyl (Fmoc) which replaces the lipid Oct chain and Leu-OMe (OMe, methoxy) as a substitute for the C-terminal Lol unit. By steady state fluorescence and circular dichroism measurements we postulated the existence of a different F0TrOMe conformation after the Tb (III) ion binding and we obtained an approximate value of the distance between the Fmoc and the Tb (III) ion. Indeed, beyond all of the promising applications of the Tb(III) ion complexes as photonic materials, an additional advantage of using Tb(III) ions in the study of F0TrOMe binding, is the possibility to characterize the TrGA conformational properties by fluorescence spectroscopy techniques. However, in that conference proceeding[34] we did not show any of the experimental results obtained, due to the shortness of this kind of contribution, and we only described our results in term of steady state fluorescence. Nevertheless steady state fluorescence makes possible to obtain only mean values on the systems investigated, without distinguishing, for example, between different peptide conformations. In addition a very important contribution on the energy transfer may come from the Fmoc triplet state and this possibility has never been explored before. For all these reasons, in this work we have decided to deepen our understanding of the F0TrOMe/Tb(III) ion complex, investigating and discussing in detail the photophysical properties of this system, employing also time resolved fluorescence and laser flash photolysis measurements. Our CD results, reported here for the first time, show that F0TrOMe is able to bind Tb(III) ions with high affinity and that this interaction gives rise to a conformational switch to a more compact structure. A large enhancement of the Tb(III) ion luminescence intensity produced by binding with F0TrOMe (related to an Fmoc→Tb(III) ion energy transfer process) is shown. By time resolved fluorescence and laser flash photolysis measurements we have demonstrated that this energy transfer can occur from both the Fmoc singlet and triplet excited states. In turn, we have used this system as a spectroscopic ruler to monitor the Fmoc⋯Tb(III) ion distances, essentially determined by the 3D-structure of the intervening peptide spacer, in the most populated peptide/ion conformer. Finally, the experimental results have been compared to those from molecular dynamics simulations, which have never been performed before on this system.

MATERIALS AND METHODS

Extraction from natural sources, chemical syntheses by solution methods, and full characterizations for native TrGA and its two analogs were already reported.[6,22,34,35]

A 40% Tb(III) perchlorate aqueous solution was obtained from Sigma-Aldrich, St. Louis (MO). Spectrograde solvents (Carlo Erba, Rodano, Italy) were exclusively used. UV-Vis absorption measurements were carried out on a Varian Cary 100 Scan spectrophotometer (Middelburg, The Netherlands) at room temperature. CD spectra were recorded using a J600 spectropolarimeter from Jasco (Tokyo, Japan). The temperature was controlled at 25 ± 0.1 °C with a thermostatted cuvette holder. The reported CD signals were normalized with respect to peptide molar concentrations. Steady-state fluorescence measurements were carried out by use of a Fluoromax 4 from Horiba-Jobin Yvon (France), operating in the single photon counting acquisition mode. The temperature was controlled at 25 ± 0.1 °C with a thermostatted cuvette holder. Emission spectra were collected using λ_{exc}= 265 and 350 nm, with 2 nm bandwidths for both the excitation and emission slits.

The Fmoc fluorescence quantum yield was determined by using naphthalene in cyclohexane as reference[37] *via* the equation:

$$\phi_u = \frac{A_s F_u n_u^2}{A_u F_s n_s^2} \phi_s \tag{1}$$

where A_s, A_u, F_s, F_u, ϕ_s and ϕ_u are the absorbances at the excitation wavelength, the integrated fluorescence intensities, and the fluorescence quantum yields of the standard (s) and unknown (u) compounds, respectively. For naphthalene in cyclohexane, ϕ_s=0.23±0.2.

Time-resolved fluorescence measurements were carried out on an EAI Life-Spec PS equipment (Edinburgh Analytical Instruments, Edinburgh, UK), operating in the single photon counting (SPC) mode. Excitation was achieved by a diode nanoled operating at 280 nm and keeping the emission at 370 nm. A cut-off filter (λ=295 nm) was used to minimize contamination from the scattered light. The temperature was controlled at 25 ± 0.1 °C with a thermostatted cuvette holder. Experimental decays were fitted through iterative reconvolution of discrete exponential functions or continuous lifetime distributions by using standard software licensed by Edinburgh Analytical Instruments. Transient absorption experiments were performed with an Applied Photophysics LKS60 instrument (Leatherhead, UK) by using a Quantel Brilliant B Nd:YAG Q-switched laser (Les Uils, France) for pump excitation. A fourth-harmonic generator module was employed to obtain a 266 nm excitation wavelength (4 ns pulse width; 10 mJ energy). All solutions for spectroscopic experiments were freshly prepared before measurement.

Molecular dynamics (MD) simulations were performed by using the GROMACS 4.6.7 software[38] with the AMBER03 force field[39] in which were added the topologies and parameters for acetonitrile,[40] perchlorate and terbium ions,[41] Aib residue[42] and Fmoc group.[43] MD simulations

were performed following our standard procedure: a two-time step energy minimization was initially carried out. Then, the solvent was equilibrated in a 150 ps MD at 50 K, during which the peptide atoms were position restrained. The system was gradually heated to 300 K through an 1 ns MD before the 250 ns production run. A Berendsen algorithm[44] was used for temperature ($\tau_T = 0.2$ ps) and pressure ($\tau_P = 1$ ps) couplings under isotropic conditions. A PME algorithm[45] for electrostatics with a double cut-off[46] at 1.4 nm for van der Waals interactions was applied. A time-step of 2 fs was employed. In the starting configuration, an α-helical conformation was assumed for the peptides randomly placed in a cubic box of side L=5 nm, filled with 1000 solvent molecules. For the simulations in the presence of terbium, we add one Tb(III) ion and three perchlorate anions to neutralize the solution. For each system, the simulations (each 250 ns long) were replicated three times.

RESULTS AND DISCUSSION

UV-Vis Absorption. The F0TrOMe absorption spectrum in acetonitrile (Figure 1A) is dominated by the optical transitions of the Fmoc chromophore, peaked at 220 [ε (220) = $2.16\pm0.04\cdot10^4$ M^{-1} cm^{-1}], 265 [ε (265) = $2.0\cdot10^4$ M^{-1}cm^{-1}], 288 [ε (288) = $6.1\cdot10^3$ M^{-1}cm^{-1}], and 299 nm [ε (299) = $6.7\cdot10^3$ M^{-1}cm^{-1}].[20,47]

Much more complicated is the absorption spectrum of Tb(ClO$_4$)$_3$ in the same solvent (Figure 1B). The optical properties of Tb(III) ions have been characterized by Carnall *et al.* in aquo-Tb (III) ion complexes.[48] They are essentially determined by the 4f→5d transition [λ = 220 nm, ε (220) = 310 M^{-1} cm^{-1})] and several 4f→4f transitions (16 in the 200-500 nm range), which are characterized by very low molar extinction coefficients (in the order of 0.5-3 M^{-1} cm^{-1}), as they are forbidden by the Laporte rule.[49-52]

Tb(ClO$_4$)$_3$ in acetonitrile shows, besides the 4f→5f band peaked at 225 nm [ε (225) = 303 M^{-1} cm^{-1}], several very weak transitions between 250 and 500 nm [^{7}F$_6$→^{5}I$_6$: λ_{max} = 265 nm, ε (265) = 0.92 M^{-1}cm^{-1}; ^{7}F$_6$→^{5}L$_9$: λ_{max}=352 nm, ε (352) = 0.30 M^{-1}cm^{-1}; ^{7}F$_6$→^{5}L$_{10}$: λ_{max} = 369 nm, ε (369) = 0.65 M^{-1}cm^{-1}] (Figure 1B, inset).
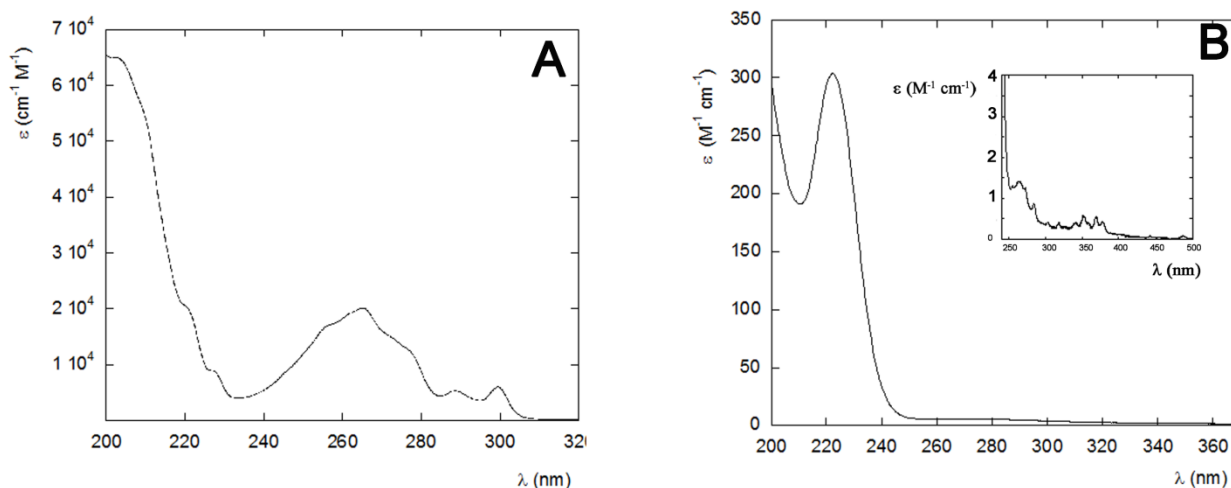
FIGURE 1 UV absorption spectra of (**A**): F0TrOMe and (**B**): $Tb(ClO_4)_3$, both in acetonitrile solution; inset: zoom in the 250-500 wavelength range.

Circular Dichroism. The CD spectrum of F0TrOMe in acetonitrile, reported in Figure 2, exhibits a strong negative band at 204 nm and a weaker negative band at 222 nm, typical of the right-handed 3_{10}-helix conformation.[53] In this secondary structure, the expected $[\Theta]_{222}/[\Theta]_{207}$ R ratio is 0.3-0.4, close to the $R = 0.22$ value found here. Moreover, this spectrum is very similar to that of TrGA, suggesting that the Fmoc chromophore does not interfere significantly with the peptide CD signal (probably because the closest chiral carbon atom, that of Leu^3, is many covalent bonds away) and does not influence the conformational features of the natural peptide either (Figure S1, Supporting Information).

Interestingly, by adding increasing amounts of Tb(III) ions to the peptide solution, a remarkable change in the CD spectrum of F0TrOMe is seen. In particular, a strong positive CD band centered at 214 nm, which exhibits increasing molar ellipticity values upon enhancing the ion molar concentration, can be readily observed (Figure 2).
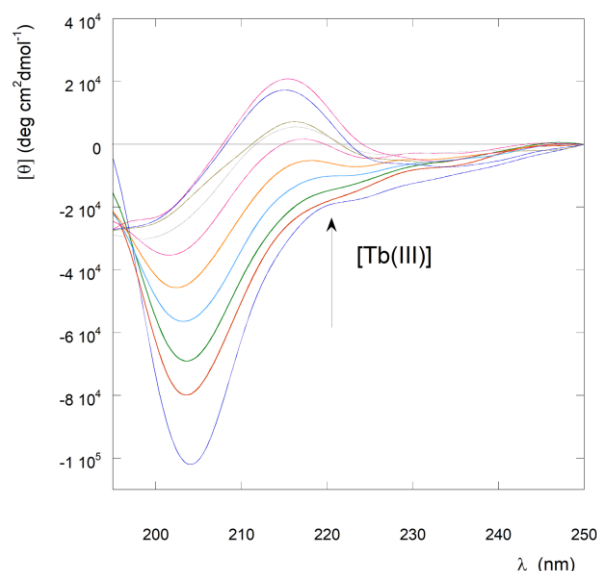
FIGURE 2 CD spectra of F0TrOMe in acetonitrile with increasing concentrations of Tb(III) ions; [F0TrOMe]=5•10[-6] M, [Tb(III)] = (0.5-6)•10[-6] M.

This finding indicates that this TrGA analog is able to bind Tb(III) ions. In particular, the CD curve obtained at the highest Tb(III) concentration value suggests the onset of a type-II β-bend local conformation.[54,55] In turn, this observation may indicate that the binding of Tb(III) ions to the peptide would produce a significant conformational transition. However, a possible direct contribution of the Tb(III) ion to the optical activity, due to the binding to the chiral F0TrOMe molecule, cannot be excluded. The spectral change after Tb(III) ion addition makes possible to determine the Tb(III)/F0TrOMe complex dissociation constant, according to equation 2.[56]

$$\frac{[\theta]_0-[\theta]}{[\theta]_0-[\theta]_\infty} = \frac{[P]+[L]+K_d-\sqrt{([P]+[L]+K_d)^2-4[P][L]}}{2[P]} \tag{2}$$

This equation refers to the formation of a 1: 1 complex between the peptide and the ligand, where $[\Theta]_0$ represents the initial molar ellipticity value of the peptide, $[\Theta]$ the molar ellipticity measured after each titrant addition, and $[\Theta]_\infty$ the molar ellipticity of the pepide-Tb(III) complex. K_d is the dissociation constant of the complex and can be interpreted as a measure of the affinity of the peptide for the ion. [P] identifies the initial concentration of the peptide (in this case 5 μM) and [L] is the concentration of the added ligand.

By plotting $([\theta]_0-[\theta])/([\theta]_0-[\theta]_\infty)$ as a function of the [Tb(III)] concentration (Figure 3), the value of dissociation constant obtained for the F0TrOMe-Tb(III) complex is $(3.6 \pm 1.0) \cdot 10^{-8}$ M. This value is comparable to the one obtained for peptides specifically designed to have high terbium binding affinity,[57,58] with binding free energy of peptide-metal complex of -42 kcal/mol.
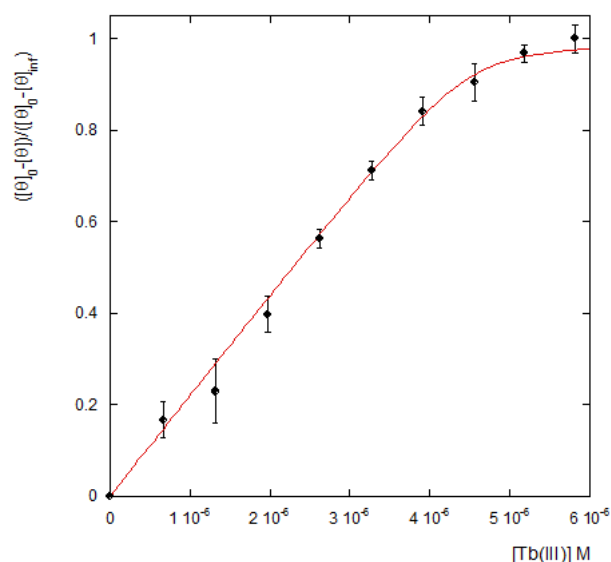
FIGURE 3. Metal titrations of Tb (III) binding peptide. Relative variation of the CD molar ellipticity at λ=214 nm in acetonitrile, T=25°C, in response to various Tb(III) ion concentrations. Peptide concentration: 5 μM.

The selectivity of the F0TrOMe/Tb(III) ion interaction is confirmed by the CD titration experiment carried out with the monovalent K^+ ion at the same ionic strength. In this case, the CD spectrum of F0TrOMe is unperturbed upon ion addition (results not shown).

We already reported similar experiments concerning the interaction of F0TrOMe with Gd(III) and Ca(II) ions, which showed the same behavior as that of Tb(III) ions.[26] Interestingly, the titration with the Gd(III) ions produced a positive CD band very similar in shape and intensity to the corresponding band recorded for the F0TrOMe/Tb(III) ion complex. On the contrary, the positive CD band of the F0TrOMe/Ca(II) ion complex is less intense and slightly red-shifted with respect to those obtained for the complexes with the trivalent Gd(III) and Tb(III) ions. These results confirm that different ions can give rise to a different conformational reorganization of the peptide chain.

Fluorescence and Resonance Energy Transfer. Beyond the possible photonic applications of the F0TrOMe/Tb(III) ion complex, the great advantage of chelating Tb(III) lanthanide ions with the F0TrOMe is the possibility to exploit photophysical techniques to obtain the experimental distance values between the Fmoc group and the Tb(III) ion. One of the earliest studies employing lanthanides as luminescent biochemical probes demonstrated the enhanced Tb(III) ion emission due to energy transfer from a Tyr residue of a membrane protein.[59] The Förster energy transfer mechanism (FRET) requires that the fluorescence of a donor moiety (the Fmoc group in our system) would overlap the absorption of an acceptor group [Tb(III)]. The FRET process can occur from both the singlet and triplet excited states of the donor molecule, the latter after singlet to triplet internal interconversion.

As far as the Fmoc singlet excited state is concerned, the emission spectrum of F0TrOMe in acetonitrile features two intense maxima at λ_{em}=301 and 310 nm (Figure S2, Supporting Information), with a fluorescence quantum yield (ϕ) of 0.34. The absorption spectrum of $Tb(ClO_4)_3$ overlaps the Fmoc fluorescence in the whole emission range (Figure S3, Supporting Information), confirming the possibility of FRET from this state. From the spectroscopic properties, it is possible to determine the Förster distance R_0, *i.e.* the distance at which the energy transfer efficiency is 0.5. For the Fmoc/Tb(III) ion pair the R_0 experimentally determined is 4.9 Å (Supporting Information). FRET from the singlet excited state induces both a decrease of the donor fluorescence and an increase of the acceptor fluorescence. However, the increase of Tb(III) ion luminescence may be also produced by FRET from the triplet excited state.[60] To demonstrate the Tb(III) ion binding to the peptide and the Fmoc sensitizing properties through FRET processes, we have recorded the Tb(III) ion luminescence spectrum by adding different amounts of F0TrOMe.

The emission spectrum of aquo-Tb(III) ion has been found to be rather complex, paralleling the complexity of its absorption spectrum. In water, the luminescence occurs from the 4f $^5D_4$ level, decaying to the seven ^7F_J states [λ=490 (J=1), 545 (J=2), 590 (J=3), 620 (J=4), 650 (J=5), 670 (J=6), and 680 nm (J=7)].[61,62] Each of these emission bands can be split or shifted by the ligand field. However, lanthanide luminescence signals are very low, due to their limited capability of absorbing light (very low molar extinction coefficient values, as reported earlier). For this reason, a sensitizing chromophore, called "antenna", is in general incorporated into the Tb(III) ion-coordinated ligand, thus allowing enhanced Tb(III) ion emission through an energy transfer process.[27-33]

In acetonitrile, by exciting the sample at 265 nm, we identified four narrow transitions, at 486, 542, 582, and 617 nm, respectively, associated to the $^5D_4 \rightarrow {}^7F_5$ manifold decay (Figure S4, Supporting Information). Interestingly, by adding F0TrOMe to a Tb(III) ion acetonitrile solution, a strong enhancement of the Tb(III) ion luminescence can be observed (Figure 4). This finding can be ascribed to two concomitant effects related to the ion coordination by F0TrOMe: a) release of solvent molecules from the coordination sphere of the ion upon association with the peptide, b) efficient energy transfer from the Fmoc moiety. The first effect has been confirmed by performing the same titration with the TrOMe analog lacking the N-terminal Fmoc chromophore (Table 1, Figure S5, Supporting Information). Also in this case an enhancement of Tb(III) ion luminescence is shown upon binding.
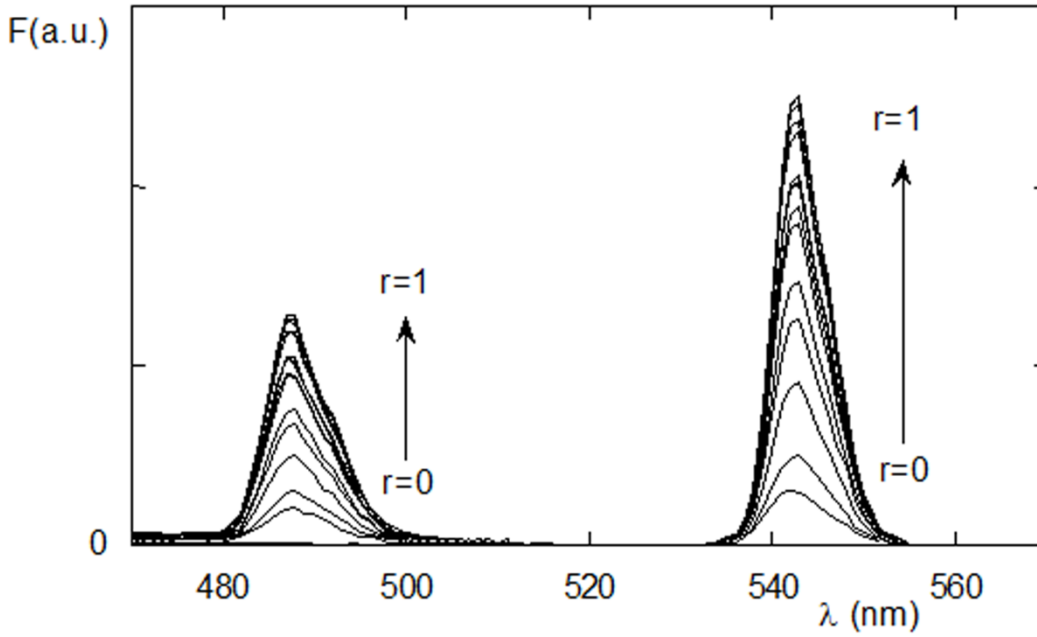
FIGURE 4 Enhancement of Tb(III) ion emission in acetonitrile by addition of F0TrOMe. The peptide/ion ratio (r) varies from 0 to 1 and λ_{exc}=265 nm.

The same experiment has been performed by exciting a Tb(III) ion solution in acetonitrile (with and without the peptide) at 350 nm, where the Fmoc chromophore does not absorb, and therefore cannot give rise to energy transfer. The luminescence intensity of the Tb(III) ions is proportional to their extinction coefficient at the excitation wavelength [$\varepsilon_A(\lambda_{exc})$], luminescence quantum yield (ϕ_A), and molar concentration C_A:

$$F_A \propto \varepsilon_A\left(\lambda_{exc}\right)\phi_A C_A \tag{3}$$

By adding different amounts of peptide, the Tb(III) ion luminescence intensity becomes:

$$F_A \propto \varepsilon_A\left(\lambda_{exc}\right)\phi_A C_{A,f} + \varepsilon_A\left(\lambda_{exc}\right)\phi_A^{'} C_{A,b} \tag{4}$$

where $C_{A,f}$ is the concentration of the free Tb(III) ions, $C_{A,b}$ is the concentration of the bound Tb(III) ions, and ϕ_A' is the luminescence quantum yield of the coordinated Tb(III) ions. At the plateau of the titration curve, where all of the Tb(III) ions are expected to be bound to F0TrOMe, the F_A[(F0TrOMe-Tb(III) ion]/F_A(Tb(III) ion ratio is 5.2, indicating that the peptide coordination causes a five times increase of the Tb(III) ion quantum yield (ϕ'_A=5ϕ_A). This result confirms a tight peptide coordination to the metal ion, removing solvent molecules from the inner coordination shell of the metal ion.

Using the 265 nm excitation wavelength, instead, both the Fmoc and Tb(III) ions can be concomitantly excited. Under these experimental conditions the acceptor luminescence intensity would include an additional contribution arising from the excitation energy transferred from the Fmoc donor. This term would be proportional to the donor extinction coefficient at the excitation

wavelength [$\varepsilon_D(\lambda_{exc})$], the acceptor quantum yield in the presence of the donor (ϕ'_A) and the energy transfer efficiency E_{ET}:

$$F_A^{(D)} \propto \varepsilon_A(\lambda_{exc})\phi_A C_{A,f} + \varepsilon_A(\lambda_{exc})\phi'_A C_{A,b} + \varepsilon_D(\lambda_{exc})C_{D,b}\phi'_A E_{ET} \tag{5}$$

At the plateau of the titration curve, the ratio F_A[(F0TrOMe-Tb(III) ion] / F_A(Tb(III) ion becomes 36, indicating that the emission of Tb(III) ions measured by excitation at 265 nm can be mostly ascribed to the Fmoc→Tb(III) ion energy transfer (Figure 5). This observation is related to the large difference in the molar extinction coefficients at 265 nm between the two chromophores [ε_{265} = 2.0·10^4 M^{-1}cm^{-1} for the Fmoc and ε_{265} = 0.92 M^{-1}cm^{-1} for the Tb(III) ions] and demonstrates the remarkable efficiency of the Fmoc group as an "antenna" chromophore, enhancing Tb (III) ion emission through the energy transfer process.
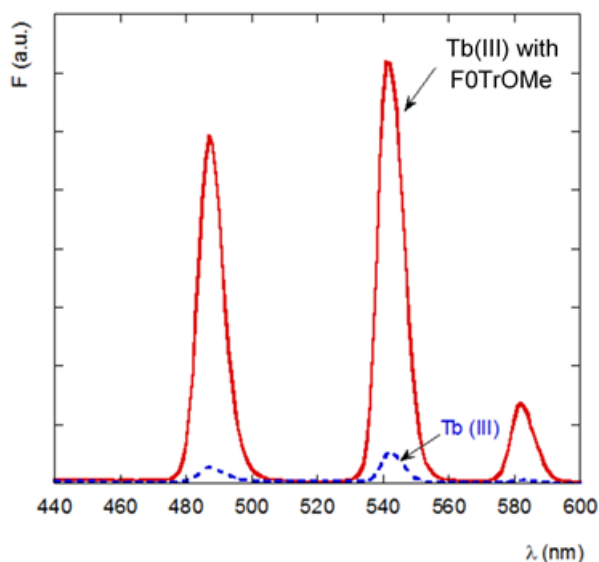

FIGURE 5 Luminescence spectra in acetonitrile of Tb(III) ions in the presence of F0TrOMe at 25 °C, by exciting at λ_{exc}=265 nm the Tb(III) ions alone (blue, dashed line) and the F0TrOMe-Tb(III) ion complex (red, full line).

A second evidence proving the FRET process can be obtained measuring the excitation spectra of Tb(III) ions in the presence or absence of the peptide at λ_{em}=542 nm (Figure 6). As clearly shown, the excitation spectrum of Tb(III) ions in acetonitrile highlights the Fmoc contribution in the wavelength range 240-310 nm. This result unequivocally demonstrates that an Fmoc→Tb(III) ion FRET mechanism is operative. For clarity, also the absorption spectra of the peptide and the metal ions are reported in Figure 6.
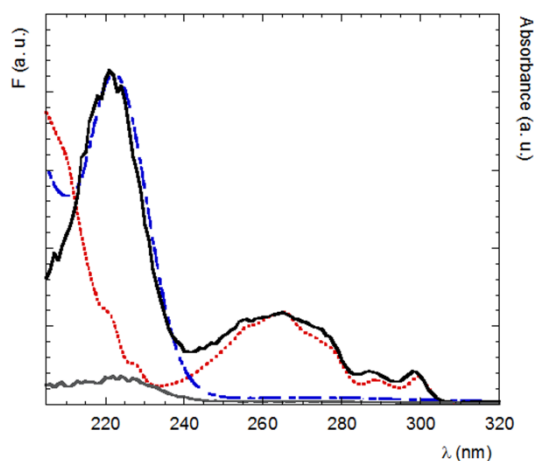
FIGURE 6 Fluorescence excitation spectrum in acetonitrile of Tb(III) ions in the presence (black line) and absence (gray line) of F0TrOMe at 5 °C (λ_{em}= 542 nm). The absorption spectra of F0TrOMe (red) and Tb(III) ions (blue) in acetonitrile are also shown.

A fluorescence titration has been also performed by adding the Tb(III) ion to an F0TrOMe acetonitrile solution (Figure 7). By plotting $(F-F_0)/(F_\infty-F_0)$ as a function of the [Tb(III)] concentration, the value of dissociation constant obtained for the F0TrOMe -Tb(III) complex is $(2.6 \pm 0.9) \cdot 10^{-8}$ M, which is comparable, within the experimental error, to the one obtained by CD measurements.
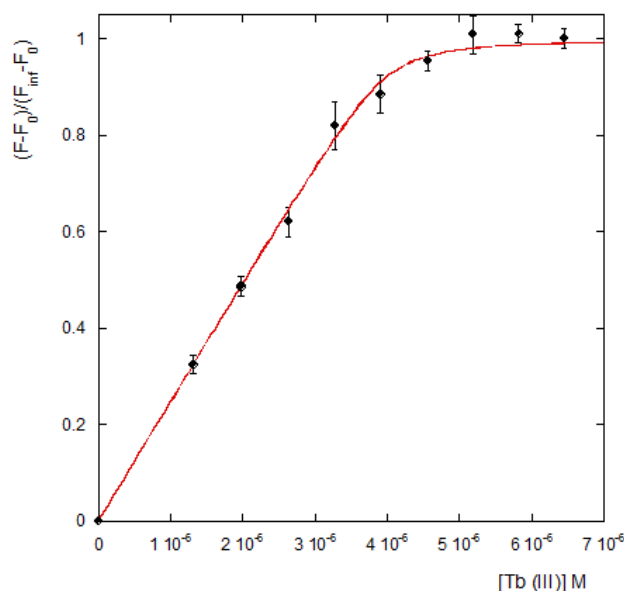

FIGURE 7 Metal titrations of Tb (III) binding peptide. Relative variation of the Tb (III) luminescence at λ_{exc}=542 nm, T=25°C, in response to various Tb(III) ion concentrations. Peptide concentration: 5 μM.

Time Resolved Fluorescence. Steady-state fluorescence measurements demonstrated the great potential of the F0TrOMe-Tb(III) ion system as a supramolecular photonic device. However, we have shown that the sensitization of the lanthanide light emission may involve both the singlet and

the triplet excited states of the antenna chromophore. To obtain a deeper understanding of the quenching process, we performed time-resolved fluorescence experiments by exciting the Fmoc chromophore, with the aim at investigating the Fmoc singlet excited state contribution to the energy transfer and at discriminating among the possible different peptide conformers contributing to peptide/Tb(III) ions interactions. Indeed, each conformer is characterized by a specific distance and orientation between the donor and acceptor groups, giving rise to distinct energy transfer efficiencies (and consequently to different lifetimes). In our case, the spherical symmetry of the Tb(III) ions eliminates the orientation dependence of the ET efficiency, leaving operative the donor···acceptor distance only.[27-33]

Therefore, we analyzed the fluorescence time decay of F0TrOMe in the absence and presence of the Tb(III) ion quencher. In the former case, the F0TrOMe decay is simply described by a mono-exponential function:

$$F_D(t) = F_D(0)\, e^{-(k_r+k_{nr})t} = F_D(0)\, e^{-\frac{t}{\tau_0}} \tag{6}$$

where k_r and k_{nr} are the radiative and non-radiative rate constants, respectively, and

$$\tau_0 = \frac{1}{k_r + k_{nr}} \tag{7}$$

is the unperturbed lifetime of the Fmoc in the F0TrOMe peptide.

In this model, each term in the sum (τ_i) is associated to a single conformer of each Fmoc in the excited state, while the pre-exponential factors α_i represent their corresponding relative population.[20,56] The experimental decay is described by two discrete lifetimes:

In the presence of the Tb(III) ion quencher, however, the F0TrOMe singlet state decay may be affected by the additional energy transfer relaxation pathway described by the function

$$F_D(t) = F_D(0)\, e^{-(k_r+k_{nr}+k_{ET})t} = F_D(0)\, e^{-\frac{t}{\tau}} \tag{8}$$

where k_{ET} is the energy transfer rate constant, and

$$\tau = \frac{1}{k_r + k_{nr} + k_{ET}} \tag{9}$$

is the lifetime of F0TrOMe in the presence of the quencher group.

The energy transfer rate constant can be easily obtained by measuring the unperturbed and quenched decays of the donor molecule

$$k_{ET} = \frac{1}{\tau} - \frac{1}{\tau_0} \tag{10}$$

In the case of the presence of multiple conformers, the decay profiles may be fitted following two different procedures, which have two different physical interpretation. The first is a multi-exponential analysis (ME). In this kind of analysis, the time-decay of $F_D(t)$ *vs.* t is fitted by the following function:

$$F_D(t) = F_D(0) \sum_i \alpha_i \, e^{-\frac{t}{\tau_i}}$$

(11)

If the different conformers do not interconvert on the nanosecond time scale, so that a dynamic averaging of the instantaneous relative positions of the donor and acceptor pair cannot take place, each decay time component can be associated to a specific conformer.[20] In this case, the experimental quenching efficiency of the *i*th conformer is obtained from the following equation:

$$E_i = 1 - \frac{\tau_i}{\tau_0}$$

(12)

Furthermore, the decay function will also provide the pre-exponential parameters α_i related to the population of the i*th* conformer.

However, if there are dynamic processes occurring during the excited state lifetime, the experimental time decays $I(t)$ can be described in terms of lifetime distribution (TD):[56]

$$I(t) = \int_0^\infty \alpha(\tau) \exp\left(-\frac{t}{\tau}\right) dt$$

(13)

This analysis provides the relative weights of a continuum of lifetimes. In case of several conformational substates and interconversion rates of the same order of magnitude as the excited state decay rate, fluorescence lifetime distributions may provide information on the conformational landscape and enable detection of the dynamics of the protein matrix on the picosecond/nanosecond time scale.

In Table 2, we reported the values for the time decay parameters, obtained by time-resolved fluorescence measurements of F0TrOMe in acetonitrile as a function of the Tb(III) ion/peptide molar concentration ratio *r*. The ME analysis shows that the F0TrOMe fluorescence decay at all *r* values is accounted for by a predominant ($\alpha \geq 0.9$) time component very similar to that measured in the absence of the quencher. However, a second shorter (less than 10%) lifetime is required to fit satisfactorily the experimental fluorescence decay for *r* values larger than 0.3. The TD analysis, instead, shows a mono-exponential decay at all Tb (III) concentrations, the heterogeneity of which (distribution widths) increases at higher Tb (III) ion concentrations.

TABLE 2: Time Decay Parameters of F0TrOMe for Different Tb(III) Ion/F0TrOMe Molar Concentration Ratios (r) (λ_{exc}=265 nm, λ_{em}= 320 nm).

r		α_1	τ_1 (ns)	α_2	τ_2 (ns)	$<\tau>$ (ns)^a	χ^2
0	ME	-	-	1	5.7	5.7	1.2
0	TD			1	5.7±0.3	5.7	1.2
0.26	ME	-	-	1	5.7	5.7	1.2
	TD			1	5.7±0.4	5.7	1.3
0.33	ME	0.08	3.6	0.92	5.7	5.5	1.2
	TD			1	5.6±0.4	5.6	1.2
0.72	ME	0.05	3.6	0.95	5.7	5.6	1.2
	TD			1	5.5±0.3	5.5	1.3
1.6	ME	0.11	3.3	0.89	5.7	5.5	1.3
	TD			1	5.4±0.8	5.4	1.3

^{a} $<\tau> = \alpha_1\tau_1 + \alpha_2\tau_2$

The simplest interpretation of these experimental findings is to admit the occurrence of one predominant F0TrOMe-Tb(III) conformation. In case of ME analysis, this conformation is characterized by an unperturbed lifetime compared to the F0TrOMe peptide, and the presence of a more quenched and less populated conformation is hypothesized. The TD analysis suggests the presence of only one conformation in which the Fmoc has a slight reduced lifetime compared to the one of the F0TrOMe peptide, and a higher conformational dynamics.

The energy transfer efficiencies, obtained by equation 12, makes possible to determine the donor-acceptor distances through the FRET model:[63]

$$E_{ET} = \frac{R_0^6}{R^6 + R_0^6} \tag{14}$$

Due to the symmetry of the Tb(III) ion, the χ^2 factor, taking into account the relative orientation of the donor-acceptor pair, can be safely averaged to 2/3.

The Tb(III) ion⋯Fmoc distances experimentally obtained are >12 Å for the most populated conformer in the ME analysis, and about 7.9 Å in the dynamical conformer from TD analysis.

Flash Photolysis. It has been demonstrated that many classes of ligand chromophores may undergo a rapid intersystem crossing to a triplet excited state followed by a very efficient energy transfer to a coordinated lanthanide. Also, this sensitized emission can give rise to an increase of luminescence of several orders of magnitude.[50,51] For this reason, to better characterize the photophysics of the

Fmoc-Tb(III) ion donor-acceptor pair, nanosecond flash-photolysis experiments have been carried out on the triplet state of the Fmoc chromophore. F0TrOMe shows a characteristic triplet-triplet absorption band between 320 and 400 nm, with a maximum at 370 nm.[20] Its Fmoc triplet state decays at 370 nm are reported in Figure 8 in the absence and presence of Tb(III) ions, while the associated decay parameters, *i.e.* the normalized differential absorptions ($\Delta A/A$) and the triplet decay rate constants (k_T), are listed in Table 3. It is worth noting that the triplet state population, proportional to $\Delta A/A$ at $t=0$, decreases parallel to the singlet state lifetime (confirming the energy transfer from the Fmoc singlet excited state), because of the competition between the Fmoc→Tb(III) ion energy transfer process and the Fmoc→ singlet-to-triplet intersystem crossing.

TABLE 3: Triplet-state decay parameters of F0TrOMe in acetonitrile, with and without the Tb(III) ion, (λ=370 nm).

Sample	$\Delta A/A$	k_T
F0TrOMe	0.16	$5.5 \cdot 10^4$
F0TrOMe/Tb(III)	0.12	$8.9 \cdot 10^4$

It also appears that Fmoc with Tb(III) ions undergoes a faster triplet decay as compared to the only F0TrOMe, suggesting that the Fmoc→Tb(III) ions energy transfer involves also the triplet state of Fmoc.
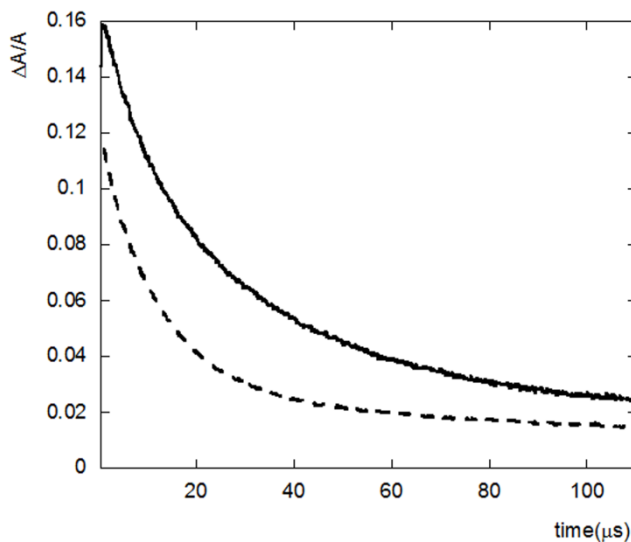

FIGURE 8 Transient absorption decays of F0TrOMe in the presence (dashed line) and absence (full line) of the Tb(III) ions (λ=370 nm, acetonitrile, 25 °C).

Molecular Dynamics Simulations. MD simulations have been performed to investigate the conformational preferences of the F0TrOMe peptide in absence and in presence of the Tb (III) ion.

Interestingly, we found that in acetonitrile the F0TrOMe peptide populate two predominant conformers, the most populated of which is a mixed $3_{10}/\alpha$- helical conformation (75% of all possible 3D-structures in our simulations, Figure 9A). This finding is in accordance with our CD experiments, with the results already published by us with similar TrGA analogs[19,24,25] and with the TrGA conformational preferences.[18,19,21-24] However, 20% of the 3D-structures found in our simulations showed a more compact and less structured conformation (Figure 9B) in which the two central, consecutive, flexible Gly residues at positions 5 and 6 allow the peptide N- and C-termini to come closer. The sum of all the other 3D-structures represented only 5%.
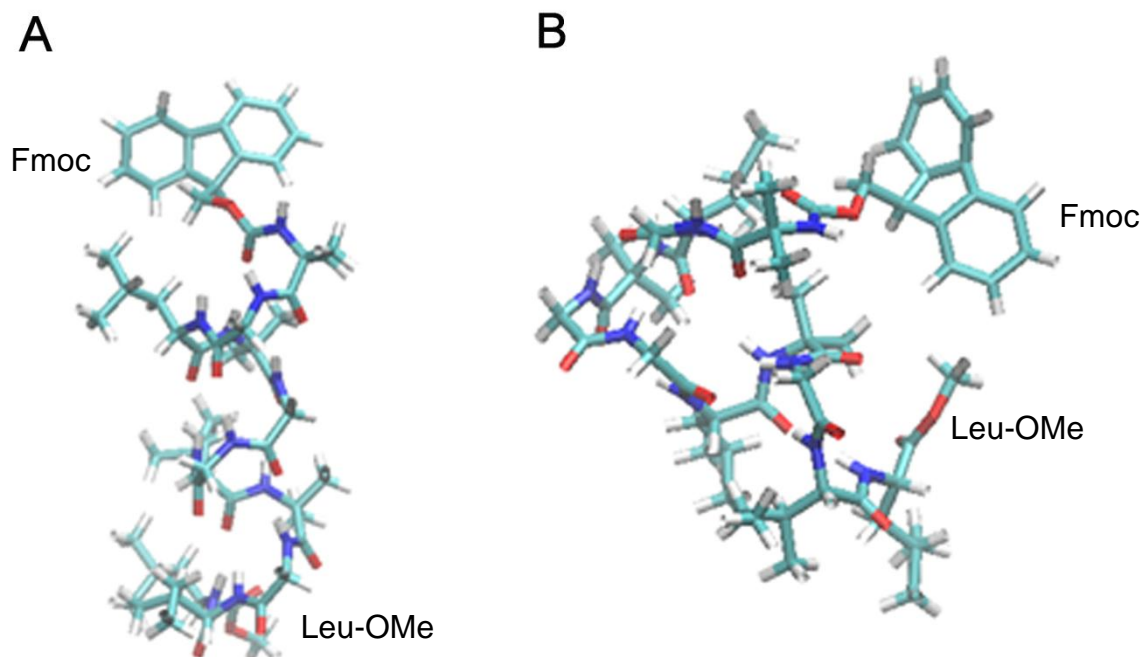

FIGURE 9 Representation of the two predominant conformers of F0TrOMe. (**A**) The predominant conformer, showing an elongated, mixed $3_{10}/\alpha$- helical conformation. (**B**) Compact 3D-structure, in which the N- and C-terminal segments are brought closer by the bend formed by the central Gly^5-Gly^6 dipeptide.

MD simulations performed in the presence of Tb(III) ions showed the capability of F0TrOMe to chelate the ion, giving rise to a conformational transition to a more compact conformer, characterized by an octa-coordinated geometry, composed of six carbonyl oxygen atoms of the peptide backbone (from N-terminus to Gly^5) and two counter ions (Figure 10), in accordance with the 8 coordination number generally found in Tb (III) complexes. The observed average Tb-O distance is (2.4±0.1) Å, while the perchlorate anions feature an average distance of (2.7±0.2) Å, typical of highly-coordinate Tb complexes, as confirmed by X-ray crystal studies on a Tb-binding peptide.[64]
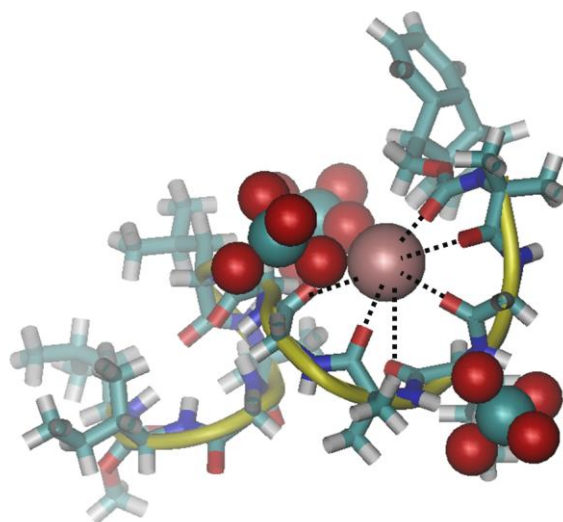
FIGURE 10 Representation of the predominant conformer of the F0TrOMe/Tb(III) ion complex.

Therefore, the conformational transition highlighted by the CD experiments could be assigned to the switch of the most populated initial peptide conformation (reported in Figure 9 A) to a different compact structures chelating the Tb(III) ion. In good agreement with the donor-acceptor distance determined by FRET experiments, the Fmoc···Tb(III) ion distance distribution in the F0TrOMe/Tb(III) ion complex is quite large, with a maximum value of (7.6 ± 0.5) Å (Figure S6, Supporting Information), in accordance to time distribution analysis.

DISCUSSION.

CD measurements shows that the binding of Tb(III) ions gives rise to a significant conformational transition of the F0TrOMe peptide from a helical structure to a bend structure. The molar ellipticity change after each Tb (III) addition makes possible to determine the dissociation constant of the complex, which has been found to be $(3.6 \pm 0.8) \cdot 10^{-8}$ M, by assuming a 1: 1 stoichiometry. The goodness of the experimental fit suggest that this stoichiometry is correct.

Steady-state fluorescence measurements show that the binding of the Tb(III) ion by the peptide causes a marked luminescence enhancement, by which, assuming the same 1:1 stoichiometry, the same K_d value was obtained: $(2.6 \pm 0.9) \cdot 10^{-8}$ M. Time resolved fluorescence experiments suggest the presence of one predominant F0TrOMe-Tb(III) conformation, characterized by an unperturbed, or only slightly decreased lifetime, depending on the kind of decay analysis. In particular, ME analysis suggests an Fmoc···Tb(III) ion distance >12 Å with low conformational dynamics, while TD analysis suggests an Fmoc···Tb(III) ion distance of 7.9 Å with quite high conformational dynamics. MD simulations shows that the F0TrOMe peptide in solution populate a most predominant conformer, characterized by a mixed $3_{10}/\alpha$- helical conformation, in accordance to CD

measurements. The MD simulation performed in the presence of Tb(III) ion shows the capability of F0TrOMe to coordinate the ion, giving rise to a conformational transition to a more compact conformer, characterized by an octa-coordinated geometry. This conformation shows a mean Fmoc⋯Tb(III) ion distance of (7.6±0.5) Å, with an heterogeneous distance distribution due to the F0TrOMe/Tb(III) ion complex dynamics, in accordance to time distribution analysis, which can be considered the most appropriate model to describe this system. Furthermore, on the basis of the CD spectra of peptide titration with metal, an almost isodichroic point can be observed, according to the equilibrium between two predominant species (free and bound peptide). The slight deviation of all the experimental curves from this point may be due both due to the presence of the other (less populated) peptide conformations and to the noise of the signal in this spectral region.

CONCLUSIONS

In conclusion, in this work we have studied, by spectroscopic techniques and MD simulations, the Tb(III) chelating properties of a TrGA analog containing the fluorescent N^{α}-protecting group Fmoc. In the past, we found that similar TrGA analogs in acetonitrile preferentially adopted a mixed $3_{10}/\alpha$-helical conformation in equilibrium with more compact structures.

MD simulations on the F0TrOMe analog, and experimental results suggest that also in this case the peptide in acetonitrile preferentially adopts a mixed $3_{10}/\alpha$- helical conformation (75% of all possible 3D-structures) in equilibrium with other 3D-structures which are more compact and have less structured conformations.

The capability of the F0TrOMe to chelate the Tb(III) ion was also investigated, using both spectroscopy experiments and MD simulations. Circular dichroism studies reveal that a conformational transition of the peptide chain takes place upon ion binding, while fluorescence experiments show that the binding of the Tb(III) ions by the peptide backbone causes a marked luminescence enhancement, due to both the release of solvent molecules from the coordination inner sphere of the ion upon association with the peptide, and the energy transfer process from the Fmoc moiety. By assuming a 1: 1 stoichiometry, the dissociation constant of the complex has been determined both from steady state and CD measurements. This value was $(3.1 \pm 0.7) \cdot 10^{-8}$ M and is comparable to the one obtained for peptides specifically designed to have high terbium binding affinity.

Time-resolved fluorescence and flash photolysis measurements highlight that Tb(III) ion sensitization can take place from both the Fmoc singlet and triplet excited states, confirming the Fmoc as a good sensitizing agent for Tb(III) ion luminescence.

Time-resolved fluorescence experiments performed in the Fmoc emission region show the occurrence, upon the Tb(III) binding, of a predominant Fmoc lifetime, which correspond to an Fmoc···Tb(III) ion distance of 7.9 Å. MD simulations shows that the F0TrOMe peptide in solution populate a most populated conformer, with a compact conformation, where the Tb(III) ion is octa-coordinate and is located at a distance of (7.6±0.5) Å from the Fmoc moiety. These values are in fair agreement with the experimental values obtained by time-resolved measurements, while the conformational changes occurring upon the ion binding are well supported by CD evidences.

Due to the Trichogin GAIV great affinity for biological membranes and its proteolytic resistance properties, these results emphasize the possible application of this very stable F0TrOMe/Tb(III) ion complex as a contrast agent for bioimaging, and bioanalytical assays based on fluorescence sensing.

REREFERENCES

[1] S. Rebuffat, C. Goulard, B. Bodo, M. T. Roquebert, *Recent Res. Devel. Org. Bioorg. Chem.* **1999**, *3*, 65.

[2] C. Toniolo, M. Crisma, F. Formaggio, C. Peggion, R. F. Epand, R. M. Epand, *Cell. Mol. Life Sci.* **2001**, *58*, 1179.

[3] H. Brückner, C. Toniolo, *Chem. Biodivers.* **2013**, *10*, 731.

[4] N. Stoppacher, N. K. N. Neumann, L. Burgstaller, S. Zeilinger, T. Degenkolb, H. Brückner, R. Schuhmacher, *Chem. Biodivers.* **2013**, *10*, 734.

[5] C. Peggion, F. Formaggio, M. Crisma, R. F. Epand, R. M. Epand, C. Toniolo, *J. Pept. Sci.* **2003**, *9*, 679.

[6] C. Avin-Guette, S. Rebuffat, Y. Prigent, B. Bodo, *J. Am. Chem. Soc.* **1992**, *114*, 2170.

[7] C. Toniolo, C. Peggion, M. Crisma, F. Formaggio, X. Shui, D. S. Eggleston, *Nat. Struct. Biol.* **1994**, *1*, 908.

[8] M. De Zotti, B. Biondi, C. Peggion, F. Formaggio, Y. Park, K. S. Hahm, C. Toniolo, *Org. Biomol. Chem.* **2012**, *10*, 1285.

[9] M. De Zotti, B. Biondi, F. Formaggio, C. Toniolo, L. Stella, Y. Park, K. S. Hahm, *J. Pept. Sci.* **2009**, *15*, 615.

[10] C. Toniolo, M. Crisma, F. Formaggio, C. Peggion, *Biopolymers* **2001**, *60*, 396.

[11] Y. Paterson, S. M. Rumsey, E. Benedetti, G. Némethy, H. A. Scheraga, *J. Am. Chem. Soc.* **1981**, *103*, 2947.

[12] V. Barone, F. Lelj, A. Bavoso, B. Di Blasio, P. Grimaldi, V. Pavone, C. Pedone, *Biopolymers* **1985**, *24*, 1759.

[13] L. Zhang, J. Hermans, *J. Am. Chem. Soc.* **1994**, *116*, 11915.

[14] R. Improta, N. Rega, C. Alemán, V. Barone, *Macrolecules* 2001, *34*, 7550.

[15] K. A. Bolin, G. L. Millhauser, *Acc. Chem. Res.* **1999**, *32*, 1027.

[16] E. Gatto, A. Porchetta, L. Stella, I. Guryanov, F. Formaggio, C. Toniolo, B. Kaptein, Q. B. Broxterman, M. Venanzi, *Chem. Biodivers.* **2008**, *5*, 1263.

[17] E. Gatto, A. Quatela, M. Caruso, R. Tagliaferro, M. De Zotti, F. Formaggio, C. Toniolo, A. Di Carlo, M. Venanzi, *ChemPhysChem* **2014**, *15*, 64.

[18] D. J. Anderson, P. Hanson, J. McNulty, G. Millhauser, V. Monaco, C. Toniolo, M. Crisma, F. Formaggio, *J. Am. Chem. Soc.* **1999**, *121*, 6919.

[19] V. Monaco, C. Toniolo, M. Crisma, F. Formaggio, X. Shui, D. S. Eggleston, *Biopolymers* **1996**, *39*, 31.

[20] M. Venanzi, E. Gatto, G. Bocchinfuso, A. Palleschi, L. Stella, F. Formaggio, C. Toniolo, *ChemBioChem* **2006**, *7*, 43.

[21] E. Gatto, G. Bocchinfuso, A. Palleschi, S. Oancea, M. De Zotti, F. Formaggio, C. Toniolo, M. Venanzi, *Chem. Biodivers.* **2013**,*10*, 887.

[22] C. Toniolo, M. Crisma, F. Formaggio, C. Peggion, V. Monaco, C. Foulard, S. Rebuffat, B. Bodo, *J. Am. Chem. Soc.* **1996**, *118*, 4952.

[23] E. Locardi, S. Mammi, C. Toniolo, M. Crisma, F. Formaggio, E. Peggion, V. Monaco, S. Rebuffat, B. Bodo, J. Kamphuis, Q. B. Broxterman, *J. Pept. Sci.* **1998**, *4*, 389.

[24] E. Locardi, S. Mammi, C. Toniolo, M. Crisma, F. Formaggio, E. Peggion, V. Monaco, S. Rebuffat, B. Bodo, *J. Pept. Res*. **1998**, *52*, 261.

[25] M. Venanzi, E. Gatto, G. Bocchinfuso, A. Palleschi, L. Stella, C. Baldini, F. Formaggio, C. Toniolo, *J. Phys. Chem. B* **2006**, *110,* 22834.

[26] M. Venanzi, G. Bocchinfuso, E. Gatto, A. Palleschi, L. Stella, F. Formaggio, C. Toniolo, *ChemBioChem* **2009**, *10*, 91.

[27] N. Sabbatini, M. Guardigli, J. M. Lehn, *Coord. Chem. Rev.* **1993**, *12*, 201.

[28] M. D. Allendorf, C. A. Bauer, R. K. Bhakta, R. J. T. Houk, *Chem. Soc. Rev.* **2009**, *38*, 1330.

[29] J. C. G. Bünzli, C. Piguet, *Chem. Soc. Rev.* **2005**, *34*, 1048.

[30] R. B. Martin, F. S. Richardson, *Q. Rev. Biophys.* **1979**, *12*, 181.

[31] F. S. Richardson, *Chem. Rev.* **1982**, *82*, 541.

[32] M. D. Allendorf, C. A. Bauer, R. K. Bhakta, R. J. T. Houka, *Chem. Soc. Rev.* **2009**, *38*, 1330.

[33] L. Armelao, S. Quici, F. Barigelletti, G. Accorsi, G. Bottaro, M. Cavazzini, E. Tondello, *Coord. Chem. Rev.* **2010**, *254*, 487.

[34] M. Venanzi, E. Gatto, L. Stella, G. Bocchinfuso, A. Palleschi, F. Formaggio, C. Toniolo, in: *Peptides for Youth. Advances in Experimental Medicine and Biology*, (Eds. S. D. Valle, E. Escher, W. D. Lubell), *611*, Springer, New York, NY, **2009**, pp. 43-44.

[35] V. Monaco, F. Formaggio, M. Crisma, C. Toniolo, P. Hanson, G. L. Millhauser, *Biopolymers* **1999**, *50*, 239.

[36] E. Gatto, C. Mazzuca, L. Stella, M. Venanzi, C. Toniolo, B. Pispisa, *J. Phys. Chem. B* **2006**, *110,* 22813.

[37] D. F. Eaton, *Pure Appl. Chem.* **1988**, *60*, 1107.

[38] S. Pronk, S. Páll, R. Schulz, P. Larsson, P. Bjelkmar, R. Apostolov, M.R. Shirts, J.C. Smith, P.M. Kasson, D. van der Spoel, B. Hess, E. Lindahl, *Bioinformatics* **2013**, *29*, 845.

[39] W. D. Cornell, P. Cieplak, C. I. Bayly, I. R. Gould, K. M. Merz, Jr., D. M. Ferguson, D. C. Spellmeyer, T. Fox, J. W. Caldwell, P. A. Kollman, *J. Am. Chem. Soc.* **1995**, *117*, 5179.

[40] A. K. Malde, L. Zuo, M. Breeze, M. Stroet, D. Poger, P. C. Nair, C. Oostenbrink, A. E. Mark, *J. Chem. Theory Comput.* **2011**, *7*, 4026.

[41] P. Li, L. F. Song, K. M. Merz, Jr., *J. Phys. Chem. B* **2015**, *119*: 883.

[42] G. Bocchinfuso, P. Conflitti, S. Raniolo, M. Caruso, C. Mazzuca, E. Gatto, E. Placidi, F. Formaggio, C. Toniolo, M. Venanzi, A. Palleschi, *J. Pept. Sci.* **2014**, *20*, 494.

[43] X. Mu, K. M. Eckes, M. M. Nguyen, L. J. Suggs, P. Ren, *Biomacromolecules* **2012**, *13*, 3562.

[44] H. J. C. Berendsen, J. P. M. Postma, W. F. van Gunsteren, A. Di Nola, J. R. Haak, *J. Chem. Phys.* **1984**, *81*, 3684.

[45] T. Darden, D. York, L. Pedersen, *J. Chem. Phys.* **1993**, *98*, 10089.

[46] D. Hamelberg, J. Mongan, J.A. McCammon, *J. Chem. Phys.* **2004**, *120*, 11919.

[47] J. Savig, A. Yoger, Y. Mazur, *J. Am. Chem. Soc.* **1977**, *12*, 6861.

[48] W. T. Carnall, P. R. Fields, K. Rajnak, *J. Chem. Phys.* **1968**, *49*, 4447.

[49] J. P. Leonard, T. Gunnlaugsson, *J. Fluoresc.* **2005**, *15*, 585.

[50] W. T. Carnall, *Handbook on the Physics and Chemistry of Rare Earths*, Vol. 3 (Eds.: K. A. Gschneider, L. Eyring), North-Holland, Amsterdam **1979**, pp 171-208.

[51] D. Parker, R. S. Dickins, H. Puschmann, C. Crossland, J. A. K. Howard, *Chem. Rev.* **2002**, *102*, 1977.

[52] D. Parker, J. A. G. Williams, *J. Chem. Soc., Dalton Trans.* **1996**, *18*, 3613.

[53] C. Toniolo, A. Polese, F. Formaggio, M. Crisma, J. Kamphuis, *J. Am. Chem. Soc.* **1996***, 113*, 2744.

[54] C. Toniolo, F. Formaggio, R. W. Woody, in *Comprehensive Chiroptical Spectroscopy*, (Eds.: N. Berova, P. L. Polavarapu, K. Nakanishi, R. W. Woody), Wiley, Hoboken (NJ) **2012**, pp. 499-544.

[55] A. Perczel, M. Hollosi, B. M. Foxman, G. D. Fasman, *J. Am. Chem. Soc.* **1991**, *113*, 9772.

[56] R. Lettieri, M. D'Abramo, L. Stella, A. La Bella, F. Leonelli, L. Giansanti, M. Venanzi, E. Gatto, *Spectrochim. Acta A Mol. Biomol. Spectrosc.* **2018**, *195*, 84.

[57] M. Nitz, K. J. Franz, R. L. Maglathlin, B. Imperiali, *ChemBioChem* **2003**, *4*, 272.

[58] C. W. am Ende, H. Y. Meng, M. Ye, A. K. Pandey, N. Zondlo, *ChemBioChem* **2010**, *11*, 1738.

[59] R. B. Mikkelsen, D. F. H. Wallak, *Biochim. Biophys. Acta* **1974**, *363*, 211.

[60] W. C. Galley, L. Stryer, *Biochemistry* **1969**, *8*, 1831.

[61] M. Petersheim, in *Biophysical and Biochemical Aspects of Fluorescence Spectroscopy* (Ed.: T.G. Dewey), Plenum Press, New York **1991**, pp 43-71.

[62] W. D. Jr. Horrocks, M. Albin, *Prog. Inorg. Chem.* **1984**, *31*, 1.

[63] J. R. Lakowicz, *Principles of Fluorescence Spectroscopy*, Third Edition, Springer, New York **2006**.

[64] M. Nitz, M. Sherawat, K. J. Franz, E. Peisach, K. N. Allen, B. Imperiali, *Angew. Chem. Int. Ed.* **2004**, *43*, 3682.